Journal of Computational Physics 524 (2025) 113724

Contents lists available at ScienceDirect

Journal of Computational Physics

journal homepage: www.elsevier.com/locate/jcp

Short note

A simple approach to derive Riemann solvers for the compressible Euler equations in the ALE formulation from their Eulerian counterpart

V. Chicu [a,b], A. Beccantini [a,*], M. Gherardi [b]

[a] Université Paris Saclay, CEA, Service d'Études Mécaniques et Thermiques, 91191, Gif-sur-Yvette Cedex, France
[b] Alma Mater Studiorum-Universitá di Bologna, Dipartimento di Ingegneria Industriale, 40136, Bologna, Italy

ARTICLE INFO

Keywords:
Euler equations
Galilean invariance
Arbitrary Lagrangian-Eulerian formulation
Approximate Riemann solvers
HLLC
AUSM$^+$

ABSTRACT

In this paper, a new formula for the inviscid flux vector of the compressible Euler equations is proposed which links its Arbitrary Lagrangian-Eulerian (ALE) and Eulerian forms. On the one hand, this formula can be applied to compute approximate Riemann solvers in the ALE formulation starting from their Eulerian version. On the other hand, as shown, the same formula is also useful to verify the correctness of an Riemann solver in the ALE formulation once its Eulerian version is given.

1. Introduction

In the last decades, shock–capturing numerical methods have been widely used to solve time–dependent hyperbolic conservation laws in different fields. They are usually based on Riemann solvers which, after the seminal work of Godunov [1], have been the subject of several research works (see [2] and references therein). Most of them are designed in the Eulerian framework,[1] with the inconvenient that when using arbitrary Lagrangian Eulerian (ALE) formulation [4] they should be redesigned.

In this document, after introducing the conservative variables and flux vector definitions (Sec. 2), in Sec. 3 we propose a formula which allows to derive, starting from its Eulerian counterpart, a Riemann solver in the direct[2] ALE formulation. As shown in Sec. 4, the Riemann solver thus obtained preserves the Galilean invariance. Using this formula, in Sec. 5 we investigate two approximate Riemann solvers in the ALE formulation presented in Luo's paper [6]: AUSM$^+$ and HLLC. As we will show, the proposed expression for the HLLC solver presents an error. The numerical experiments investigated in Sec. 6 support that the new formula gives, for the HLLC solver in the ALE formulation, the same results as the classic one. Conclusion follows.

* Corresponding author.
E-mail address: alberto.beccantini@cea.fr (A. Beccantini).

[1] Only a few authors have designed Riemann solvers adopting the Lagrangian standpoint before designing their Eulerian counterpart, despite of the benefits that would come with it [3].

[2] In direct ALE formulation, advective terms are explicitly included in governing equations, opposite to indirect ALE approach, which involves a Lagrangian stage [5].

https://doi.org/10.1016/j.jcp.2025.113724
Received 28 March 2024; Received in revised form 21 December 2024; Accepted 4 January 2025

Available online 9 January 2025

2. Definitions

The governing equations for the ALE formulation are presented, for instance, in Sec. 2 of [6]. A part a few exceptions (see for instance [7,8] and reference therein), they are solved using shock capturing approaches based on 1D Riemann solvers. Then, as pointed out in Sec. 3.2.4 of [2] and in Sec. 3 of [9], without loss of generality we can restrict our attention to the 1D case.

We define the (one-dimensional) conservative variables in the fixed frame and in the moving boundary frame as:

$$\mathbf{U} = \begin{pmatrix} \rho \\ \rho v \\ \rho E \end{pmatrix}, \quad \tilde{\mathbf{U}} = \begin{pmatrix} \rho \\ \rho \tilde{v} \\ \rho \tilde{E} \end{pmatrix} = \begin{pmatrix} \rho \\ \rho(v - \dot{x}) \\ \rho e + \frac{1}{2}\rho(v - \dot{x})^2 \end{pmatrix}, \tag{1}$$

where ρ is the density, v the flow velocity, $\dot{x}$ is the boundary speed, and E the specific total energy, defined by

$$E = e + \frac{1}{2}v^2,$$

i.e. involving the specific internal energy e and the kinetic one.

We also distinguish between flux vector in the ALE and Eulerian formulation:

$$\mathbf{F}_{\mathrm{ALE}} = (v - \dot{x})\mathbf{U} + P\begin{pmatrix} 0 \\ 1 \\ v \end{pmatrix}, \quad \mathbf{F}_{\mathrm{E}} = v\mathbf{U} + P\begin{pmatrix} 0 \\ 1 \\ v \end{pmatrix}, \tag{2}$$

P being the pressure.

3. A bridge formula between Eulerian and ALE formulation

Using (2), we can write the Eulerian flux in the boundary frame as:

$$\tilde{\mathbf{F}} = (v - \dot{x})\begin{pmatrix} \rho \\ \rho(v - \dot{x}) \\ \rho e + \frac{1}{2}\rho(v - \dot{x})^2 \end{pmatrix} + P\begin{pmatrix} 0 \\ 1 \\ (v - \dot{x}) \end{pmatrix}. \tag{3}$$

By observing that

$$\frac{1}{2}(v - \dot{x})^2 = \frac{1}{2}v^2 + \frac{1}{2}\dot{x}^2 - \dot{x}v = \frac{1}{2}v^2 - \dot{x}(v - \dot{x}) - \frac{1}{2}\dot{x}^2, \tag{4}$$

after straightforward calculations it can be written that

$$\begin{aligned} \tilde{\mathbf{F}} &= \underbrace{(v - \dot{x})\begin{pmatrix} \rho \\ \rho v \\ \rho e + \frac{1}{2}\rho v^2 \end{pmatrix} + P\begin{pmatrix} 0 \\ 1 \\ v \end{pmatrix}}_{\mathbf{F}_{\mathrm{ALE}}} - (v - \dot{x})\begin{pmatrix} 0 \\ \rho\dot{x} \\ 0 \end{pmatrix} \\ &\quad - \dot{x}\begin{pmatrix} 0 \\ 0 \\ P \end{pmatrix} - (v - \dot{x})\begin{pmatrix} 0 \\ 0 \\ \rho\dot{x}(v - \dot{x}) \end{pmatrix} - (v - \dot{x})\begin{pmatrix} 0 \\ 0 \\ \frac{1}{2}\rho\dot{x}^2 \end{pmatrix} \\ &= \mathbf{F}_{\mathrm{ALE}} - \underbrace{\rho(v - \dot{x})}_{(\tilde{\mathbf{F}})_1}\begin{pmatrix} 0 \\ \dot{x} \\ \frac{1}{2}\dot{x}^2 \end{pmatrix} - \underbrace{\left(P + \rho(v - \dot{x})^2\right)}_{(\tilde{\mathbf{F}})_2}\begin{pmatrix} 0 \\ 0 \\ \dot{x} \end{pmatrix} \end{aligned}$$

where $\left(\tilde{\mathbf{F}}\right)_i$ is the i-th component of $\tilde{\mathbf{F}}$. In compact form,

$$\mathbf{F}_{\mathrm{ALE}} = \tilde{\mathbf{F}} + \left(\tilde{\mathbf{F}}\right)_1\begin{pmatrix} 0 \\ \dot{x} \\ \frac{1}{2}\dot{x}^2 \end{pmatrix} + \left(\tilde{\mathbf{F}}\right)_2\begin{pmatrix} 0 \\ 0 \\ \dot{x} \end{pmatrix}. \tag{5}$$

$\mathbf{F}_{\mathrm{ALE}}$ is the inviscid flux vector in the fixed frame while $\tilde{\mathbf{F}}$ is the Eulerian inviscid flux vector expressed in the boundary frame. The first component of the formula is a consequence of the fact that the mass flux is the same in the fixed and moving frames. The second one expresses that, because of the different frame velocities, the mass entering the control volume gives an extra contribution to the momentum flux in the fixed frame with respect to the moving one. Finally, concerning the third component, we remind that the total

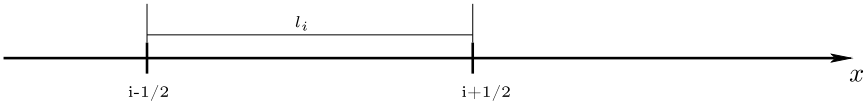

Fig. 1. Finite volume cell i.

energy is the sum of the internal energy (which is the same in both frames) and the kinetic energy (which is different because of the boundary frame velocity). Then, because of the frame relative velocity, the mass flux affects the variation of the kinetic energy while the momentum flux affects both the variation of internal and kinetic energy because of the different inertia and pressure power injection.

From a practical point of view, Formula (5) allows to compute $\mathbf{F}_{\mathrm{ALE}}$ using the Eulerian formulation of a Riemann solver, i.e. without the necessity of reprogramming its ALE version.

4. Galilean invariance in the discrete sense

Let us restrict our attention to an explicit scheme, first order accurate in space and time, and consider the finite volume cell represented in Fig. 1 (l being its time variable length). We define, on the variables a and b,

$$\Delta_i(a) = \frac{a_i^{n+1} - a_i^n}{t^{n+1} - t^n}, \quad \delta_i(b) = b_{i-1/2}^n - b_{i+1/2}^n.$$

We verify the Galilean invariance in the discrete sense of Formula (5), i.e. that

$$\Delta_i(l\mathbf{U}) = \delta_i\left(\mathbf{F}_{\mathrm{ALE}}\right) \underbrace{=}_{(5)} \delta_i\left(\tilde{\mathbf{F}} + \left(\tilde{\mathbf{F}}\right)_1 \begin{pmatrix} 0 \\ \dot{x} \\ \frac{1}{2}\dot{x}^2 \end{pmatrix} + \left(\tilde{\mathbf{F}}\right)_2 \begin{pmatrix} 0 \\ 0 \\ \dot{x} \end{pmatrix}\right) \tag{6}$$

gives the same results in fixed and constant velocity moving frames.

According to Formula (6), the density conservation in fixed and moving frames gives

$$\Delta_i(l\rho) = \delta_i\left(\left(\tilde{\mathbf{F}}\right)_1\right) \tag{7}$$

which implies that the time evolution of the density is the same in both frames.

The momentum conservation in the fixed frame gives

$$\Delta_i(l\rho v) = \delta_i\left(\left(\tilde{\mathbf{F}}\right)_2\right) + \delta_i\left(\left(\tilde{\mathbf{F}}\right)_1 \dot{x}\right). \tag{8}$$

In a frame moving with constant velocity w, the RHS of Formula (6) gives

$$\begin{aligned} \delta_i\left(\left(\tilde{\mathbf{F}}\right)_2\right) + \delta_i\left(\left(\tilde{\mathbf{F}}\right)_1 (\dot{x} - w)\right) &= \underbrace{\delta_i\left(\left(\tilde{\mathbf{F}}\right)_2\right) + \delta_i\left(\left(\tilde{\mathbf{F}}\right)_1 (\dot{x})\right)}_{\text{RHS of (8)}} - w \underbrace{\delta_i\left(\left(\tilde{\mathbf{F}}\right)_1\right)}_{\text{RHS of (7)}} \\ &= \Delta_i(l\rho v) - w\Delta_i(l\rho) = \Delta_i(l\rho(v-w)), \end{aligned}$$

which implies that the time evolution of the momentum computed using Formula (6) respects the Galilean transformation rules.

The total energy conservation in the fixed frame gives

$$\Delta_i\left(l\rho\left(e + \frac{1}{2}v^2\right)\right) = \delta_i\left(\left(\tilde{\mathbf{F}}\right)_3\right) + \delta_i\left(\left(\tilde{\mathbf{F}}\right)_1 \frac{\dot{x}^2}{2}\right) + \delta_i\left(\left(\tilde{\mathbf{F}}\right)_2 \dot{x}\right). \tag{9}$$

In a moving frame, the RHS of Formula (6) gives

$$\begin{aligned} &\delta_i\left(\left(\tilde{\mathbf{F}}\right)_3\right) + \delta_i\left(\left(\tilde{\mathbf{F}}\right)_1 \frac{(\dot{x}-w)^2}{2}\right) + \delta_i\left(\left(\tilde{\mathbf{F}}\right)_2 (\dot{x}-w)\right) = \\ &= \underbrace{\delta_i\left(\left(\tilde{\mathbf{F}}\right)_3\right) + \delta_i\left(\left(\tilde{\mathbf{F}}\right)_1 \frac{\dot{x}^2}{2}\right) + \delta_i\left(\left(\tilde{\mathbf{F}}\right)_2 \dot{x}\right)}_{\text{RHS of (9)}} \\ &- w\underbrace{\left(\delta_i\left(\left(\tilde{\mathbf{F}}\right)_1 \dot{x}\right) + \delta_i\left(\tilde{\mathbf{F}}\right)_2\right)}_{\text{RHS of (8)}} + \frac{w^2}{2}\underbrace{\delta_i\left(\tilde{\mathbf{F}}\right)_1}_{\text{RHS of (7)}} \\ &= \Delta_i\left(l\rho\left(e + \frac{1}{2}v^2\right)\right) - w\Delta_i(l\rho v) + \frac{w^2}{2}\Delta_i(l\rho) = \Delta_i\left(l\rho\left(e + \frac{1}{2}(v-w)^2\right)\right), \end{aligned}$$

which implies that the time evolution of the total energy computed using Formula (6) respects the Galilean transformation rules.

5. Examples of application: AUSM$^+$ and HLLC in the ALE formulation

As already mentioned, Formula (5) can be used to extend any Riemann solver from the Eulerian to the ALE formulation. For instance, using the Eulerian version of AUSM$^+$ [10] or HLLC (Chapter 10 of [2]), we can directly use Formula (5) to compute their ALE version in our CFD code.

Differently, Formula (5) can be used to derive the ALE expression of the Riemann solver. Proceeding in this way, in Sec. 5.1 we obtain the ALE version of AUSM$^+$ proposed in [6].

Formula (5) can also be used to verify if the implementation of the ALE expression of the Riemann solver is correct. As we will show in Sec. 5.2, the ALE version of HLLC proposed in [6] presents an error.

5.1. AUSM$^+$

The AUSM-family has been constructed with the aim of removing the numerical dissipation of the van Leer-type flux vector splittings on stationary contact/shear waves [11]. As mentioned in [10, Formula (3)], in the Eulerian formulation the inviscid flux is split into

$$\mathbf{F}_{\mathrm{E}} = \underbrace{\rho v}_{\dot{m}} \underbrace{\begin{pmatrix} 1 \\ v \\ e + \frac{1}{2}v^2 + \frac{P}{\rho} \end{pmatrix}}_{\boldsymbol{\Psi}} + \begin{pmatrix} 0 \\ P \\ 0 \end{pmatrix}.$$

Then, according to Formula (5) in [10], the numerical flux between the i-th cell (left) and the j-cell (right) is evaluated as

$$\left[\mathbf{F}_{\mathrm{E}}\right]_{i,j} = \dot{m}_{1/2}\boldsymbol{\Psi}_{i/j} + \begin{pmatrix} 0 \\ P_{1/2} \\ 0 \end{pmatrix}, \quad \boldsymbol{\Psi}_{i/j} = \begin{cases} \boldsymbol{\Psi}_i & \dot{m}_{1/2} \geq 0 \\ \boldsymbol{\Psi}_j & \dot{m}_{1/2} < 0 \end{cases} \tag{10}$$

As far as $\dot{m}_{1/2}$ and $P_{1/2}$ are concerned, different formulae are proposed (see for instance [10] and references therein).

In the ALE formulation proposed in [6] (Formula (4.8)), the inviscid flux vector is split as

$$\mathbf{F}_{\mathrm{ALE}} = \underbrace{\rho(v - \dot{x})}_{\tilde{\dot{m}}} \underbrace{\begin{pmatrix} 1 \\ v \\ e + \frac{1}{2}v^2 + \frac{P}{\rho} \end{pmatrix}}_{\boldsymbol{\Psi}} + \begin{pmatrix} 0 \\ P \\ 0 \end{pmatrix} + \begin{pmatrix} 0 \\ 0 \\ P\dot{x} \end{pmatrix},$$

which gives

$$\left[\mathbf{F}_{\mathrm{ALE}}\right]_{i,j} = \tilde{\dot{m}}_{1/2}\boldsymbol{\Psi}_{i/j} + \begin{pmatrix} 0 \\ P_{1/2} \\ P_{1/2}\dot{x} \end{pmatrix}, \quad \boldsymbol{\Psi}_{i/j} = \begin{cases} \boldsymbol{\Psi}_i & \tilde{\dot{m}}_{1/2} \geq 0 \\ \boldsymbol{\Psi}_j & \tilde{\dot{m}}_{1/2} < 0 \end{cases} \tag{11}$$

Let us now calculate the RHS of Eq. (5) using the Eulerian flux (10) in the boundary frame.

$$\begin{aligned}
&\left(\left[\tilde{\mathbf{F}}\right]_{i,j}\right)_1 = \tilde{\dot{m}}_{1/2} \\
&\left(\left[\tilde{\mathbf{F}}\right]_{i,j}\right)_2 + \dot{x}\left(\left[\tilde{\mathbf{F}}\right]_{i,j}\right)_1 &&= \tilde{\dot{m}}_{1/2}(v - \dot{x})_{i/j} + P_{1/2} + \dot{x}\left(\left[\tilde{\mathbf{F}}\right]_{i,j}\right)_1 \\
&&&= \tilde{\dot{m}}_{1/2}(v - \dot{x})_{i/j} + P_{1/2} + \dot{x}\tilde{\dot{m}}_{1/2} \\
&&&= \tilde{\dot{m}}_{1/2}(v)_{i/j} + P_{1/2} \\
&\left(\left[\tilde{\mathbf{F}}\right]_{i,j}\right)_3 + \dot{x}\left(\left[\tilde{\mathbf{F}}\right]_{i,j}\right)_2 + \frac{\dot{x}^2}{2}\left(\left[\tilde{\mathbf{F}}\right]_{i,j}\right)_1 &&= \\
&&&= \tilde{\dot{m}}_{1/2}\left(e + \frac{(v - \dot{x})^2}{2} + \frac{P}{\rho}\right)_{i/j} \\
&&&+ \dot{x}\left(\tilde{\dot{m}}_{1/2}(v - \dot{x})_{i/j} + P_{1/2}\right) + \frac{\dot{x}^2}{2}\tilde{\dot{m}}_{1/2} \\
&\underbrace{=}_{(4)} &&\tilde{\dot{m}}_{1/2}\left(e + \frac{v^2}{2} + \frac{P}{\rho}\right)_{i/j} + P_{1/2}\dot{x}
\end{aligned}$$

As one can see, the last three equations coincide with the three components of $\left[\mathbf{F}_{\mathrm{ALE}}\right]_{i,j}$ given by Formula (11).

5.2. HLLC

As we will show in Sec. 6, there is an error in Luo's formulae for the ALE version of HLLC [6]. In order to show the origin of this error, we here revisit the intermediate states formulae in the fixed (Sec. 5.2.1) and boundary frames (Sec. 5.2.2) and we show that they respect the Galilean transformation rules.

The HLLC solver is presented in details in Ch.10 of [2]. As in the previous section, and as in [6], we search for the flux between the i-th cell (left) and the j-cell (right). We indicate the fastest wave speed with S_k in the fixed frame and with $\tilde{S}_k$ in the boundary frame (with $k = i, j$). The definition of the fastest wave speed being Galilean invariant (see for instance Luo's Formulae (4.25) and (4.26) in [6] or Batten's Formula (51) in [12]), it is

$$\tilde{S}_k = S_k - \dot{x}. \tag{12}$$

In this case, since the HLLC is obtained using the Rankine-Hugoniot conditions, the HLLC approximate solution is Galilean invariant, as we will show below.

5.2.1. The intermediate states in the fixed frame

As presented in Chapter 10 of [2], in the fixed frame it is

$$S^* = \frac{\rho_j v_j \left(S_j - v_j\right) - \rho_i v_i \left(S_i - v_i\right) + P_i - P_j}{\rho_j \left(S_j - v_j\right) - \rho_i \left(S_i - v_i\right)}, \tag{13}$$

$$P^* = P_i^* = P_j^*, \tag{14}$$

with

$$P_k^* = P_k + \rho_k \left(S_k - v_k\right)\left(S^* - v_k\right) \quad , k = i, j. \tag{15}$$

Combining these formulae with Formula (10.39) of [2], one can obtain Formula (33) of [13]:

$$(\mathbf{U})_k^* = \begin{pmatrix} \rho_k^* \\ (\rho v)_k^* \\ (\rho E)_k^* \end{pmatrix} = \frac{1}{S_k - S^*} \begin{pmatrix} (S_k - v_k)\rho_k \\ (S_k - v_k)(\rho v)_k + (P^* - P_k) \\ (S_k - v_k)(\rho E)_k - P_k v_k + P^* S^* \end{pmatrix}. \tag{16}$$

We also notice that (as expected)

$$\frac{(\rho v)_k^*}{\rho_k^*} = \frac{(\rho v)_k}{\rho_k} + \frac{P^* - P_k}{S_k - S^*} \underbrace{=}_{(15)} v_k + (S^* - v_k) = S^*. \tag{17}$$

Finally the intermediate state kinetic energy and internal energy per unit volume can be expressed as

$$\begin{aligned} \frac{1}{2}(\rho v)_k^* v_k^* \quad &= \quad \frac{1}{2}(\rho v)_k^* S^* \underbrace{=}_{(16)} \frac{1}{2(S_k - S^*)} \left((S_k - v_k)(\rho v)_k S^* + (P^* - P_k) S^*\right) \\ &\underbrace{=}_{(15)} \frac{1}{S_k - S^*} \left((S_k - v_k)\frac{1}{2}\rho_k v_k^2 + \frac{1}{2}(P^* - P_k)\left(v_k + S^*\right)\right), \\ (\rho E)_k^* - \frac{1}{2}(\rho v)_k^* v_k^* \; &= \; \frac{1}{S_k - S^*} \left((S_k - v_k)\left((\rho E)_k - \frac{1}{2}\rho_k v_k^2\right)\right. \\ &+ \; \left.\frac{1}{2}(P^* - P_k)(S^* - v_k)\right). \end{aligned} \tag{18}$$

5.2.2. The intermediate states in the boundary frame

Intermediate states in the boundary frame can be computed using, in the formulae presented above (Sec. 5.2.1), the wave speeds $\tilde{S}_k$ and the velocities $\tilde{v} = v - \dot{x}$ instead of their values in the fixed frame.

Since $\tilde{S}_k - \tilde{v}_k = S_k - v_k$ and $\tilde{S}^* - \tilde{v}_k = S^* - v_k$, it follows that pressures (equations (14) and (15)), densities (Eq. (16)) as well as internal energies per unit volume (Eq. (18)), are the same in both frames. The momentum (Eq. (17)) is

$$(\rho\tilde{v})_k^* = \rho_k^* \tilde{S}^* = \rho_k^*(S^* - \dot{x}) = (\rho v)_k^* - \rho_k^* \dot{x},$$

i.e. as expected the formulae presented in Sec. 5.2.1 obey to the Galilean transformation rules.

Table 1
Initial conditions for 1D test cases. Stiffened gas (Tamman) EOS (as in [6, Sec. 5]). Case 1 one corresponds to an isolated shock wave with speed $\sigma \approx -1.9020495$ (non-dimensional values). Case 2 is a gas-water shock tube [6, Sec. 5.4] (SI values). Case 3 is the Le Blanc shock tube [3, Tab. 1] (non-dimensional values).

Case	Left state	Right state	Domain	Discont.	Final time	EOS	
	$(\rho, v, P)_{\mathrm{L}}$	$(\rho, v, P)_{\mathrm{R}}$				$\gamma_{\mathrm{L}}, \gamma_{\mathrm{R}}$	$P_{\mathrm{c,L}}, P_{\mathrm{c,R}}$
1	1 0 1	2.0443754 -0.97166778 2.8481602	-	-	-	1.4, 1.4	0, 0
2	1.271 0 $9.119252 \cdot 10^{9}$	0.999983 0 $1.01325 \cdot 10^{6}$	[0, 100]	50	$1.6 \cdot 10^{-4}$	1.4, 7	0, $3.03975 \cdot 10^{9}$
3	1 0 $2/3 \cdot 10^{-1}$	10^{-3} 0 $2/3 \cdot 10^{-10}$	[0, 9]	3	6	5/3, 5/3	0, 0

Table 2
Isolated shock wave (Table 1, Case 1). From the top to the bottom: left state, intermediate left and right states (with the fastest wave speeds), right state. Non-dimensional values.

State	ρ	v	P	ρE	S
L	1.0	0.0	1.0	2.5	-
L* [13]	2.0443754	-0.97166778	2.8481602	8.0854870	-1.9020495E
R* [13]	2.0443754	-0.97166778	2.8481602	8.0854870	0.75850087
L* [6]	2.0443754	-0.97166778	2.8481602	4.3071536	-1.9020495
R* [6]	2.0443754	-0.97166778	2.8481602	8.0854870	0.75850087
R	2.0443754	-0.97166778	2.8481602	8.0854870	-

Table 3
Isolated shock wave (Table 1, Case 1). $\mathbf{F}_{\mathrm{ALE}}$ on the left and on the right of $\dot{x} = \sigma = -1.9020495$. Non-dimensional values.

	$(\mathbf{F}_{\mathrm{ALE}})_1^{\mathrm{L}}$	$(\mathbf{F}_{\mathrm{ALE}})_1^{\mathrm{L}^*}$	$(\mathbf{F}_{\mathrm{ALE}})_2^{\mathrm{L}}$	$(\mathbf{F}_{\mathrm{ALE}})_2^{\mathrm{L}^*}$	$(\mathbf{F}_{\mathrm{ALE}})_3^{\mathrm{L}}$	$(\mathbf{F}_{\mathrm{ALE}})_3^{\mathrm{L}^*}$
Formula (5)	1.9020495	1.9020495	1.0	1.0	4.7551239	4.7551239
[13]	1.9020495	1.9020495	1.0	1.0	4.7551239	4.7551239
[6]	1.9020495	1.9020495	1.0	1.0	4.7551239	1.2398315

5.2.3. *Discussion on the Luo's formulae*

As one can see, the only difference between Eq. (16) and Luo's formulae (4.19) - (4.20) in [6] is in the evaluation of the intermediate state total energies in the fixed frame:

$$\left[(\rho E)_k^*\right]_{\mathrm{Luo}} = \frac{\tilde{S}_k - \tilde{v}_k}{\tilde{S}_k - \tilde{S}^*}(\rho E)_k - \frac{P_k \tilde{v}_k - P^* \tilde{S}^*}{\tilde{S}_k - \tilde{S}^*} = (\rho E)_k^* - \frac{(P^* - P_k)}{\tilde{S}_k - \tilde{S}^*}\dot{x}. \tag{19}$$

The error arises from the fact that Luo's formulae involve wave speeds and velocities expressed in the boundary frame. Incidentally, while the internal energy is a Galilean invariant, the total one is not, the kinetic energy being different in the fixed and boundary frames. If follows that, in the total energy formula, one should use wave speeds and velocities expressed in the fixed frame (as in Formula (18) or Formula (33) of [13]).

6. Numerical verifications

Let us now present some numerical verifications which support that, for the HLLC solver, Formula (5) and its classic ALE flux formula (for instance, van der Vegt's Formula (33) in [13]) give the same numerical results. For this purpose, the three shock tube test cases of Table 1 are considered. Case 1 is an isolated shock wave on which we simplify verify that Formula (5) and van der Vegt's formula are equal to the exact flux function at the discontinuity, thus preserving the isolated discontinuity as the mesh interface and the shock have the same speed. Cases 2 and 3 are shock tubes that are considered to be challenging for the robustness of the numerical solvers [6,3] and therefore will be computed using the two aforementioned HLLC flux formulae.

First of all, let us consider the isolated shock wave (Table 1, Case 1). If we compute the fastest wave speeds using Batten's Formula (51) in [12], the HLLC solution of the given Riemann problem coincides with the exact one. In Table 2 we present the values for the intermediate states (L* and R*) obtained using van der Vegt's Formula (33) in [13] and Luo's Formulae (4.19) - (4.20) in [6], respectively. According to van der Vegt's Formula, states L*, R* and R are identical, which confirms that we are dealing with a left isolated shock wave. Same for Luo's formula, except for the total energy per unit volume in the L* state, which is incorrect. In Table 3

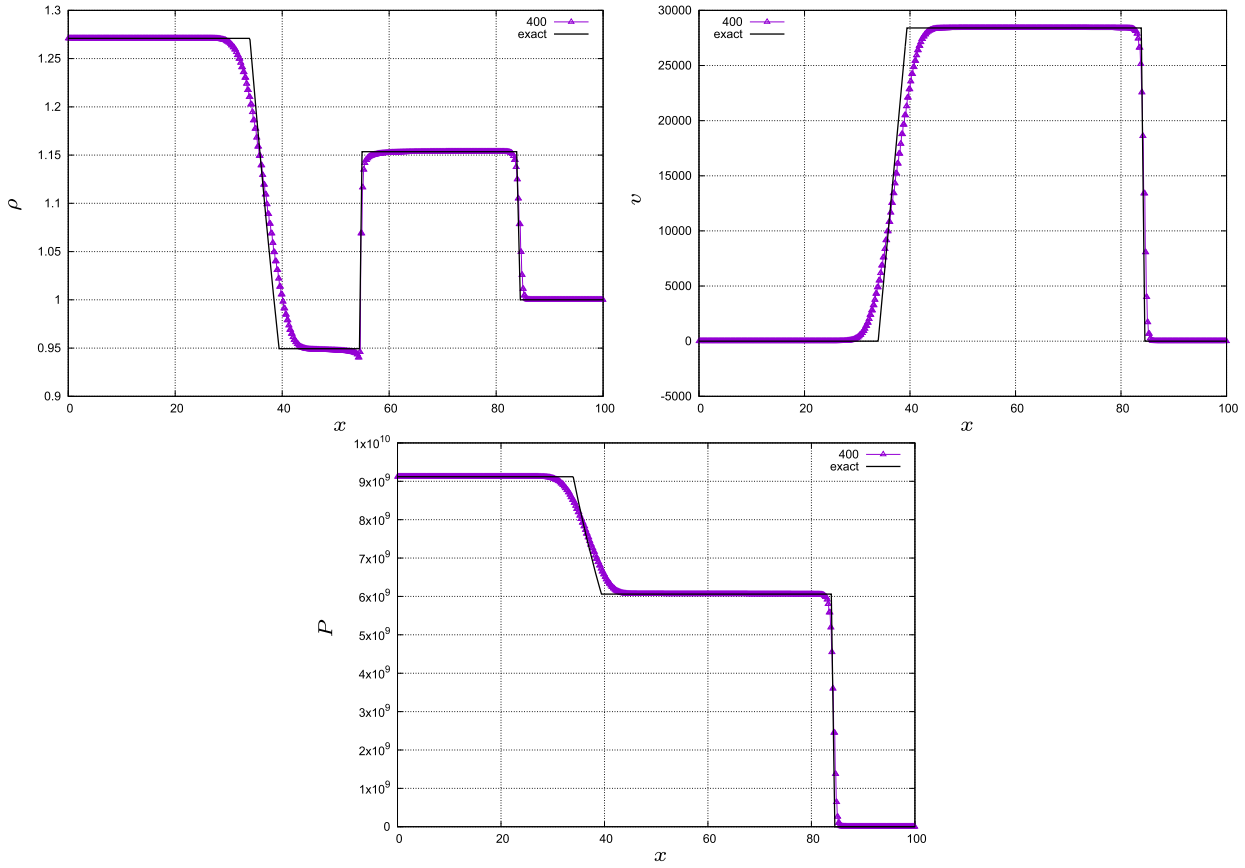

Fig. 2. Gas-water shock tube (Table 1, Case 2). SI values. HLLC computations with Formula (5).

we present the ALE HLLC fluxes evaluated on the left and on the right of the boundary travelling with speed $\dot{x} = \sigma = -1.9020495$ (i.e. on the states L and L* of the isolated shock wave Riemann problem), obtained using Formula (5), van der Vegt's formula and Luo's one. They are all identical, except for the Luo's energy flux on the right of the boundary, which is false.

Let us now compute cases 2 and 3 of Table 1 and compare the numerical results obtained using the expression of the ALE HLLC flux according to two aforementioned HLLC flux formulae. All computations are carried out using the Europlexus code [14], with an explicit ALE Cell-Centered Finite Volume algorithm which is first order accurate in space and time (with a CFL number equal to 0.45). At each time step, the velocity of the interface containing the initial discontinuity is computed as the Roe average of the flow velocity, at the previous time step, of two elements sharing the interface. All the other interfaces move to maintain a constant mesh size on the left and of the right side of the initial discontinuity.

In Fig. 2 we represent the numerical results for the gas-water shock tube (Table 1, Case 2), obtained using Formula (5) for the HLLC solver. As one can see, even with a mesh with 400 elements the numerical solution is close to the exact one. The numerical results obtained using the van der Vegt's formula are not shown here as they are almost identical to those of Fig. 2. We only mention that the computed absolute differences between the two flux formulae are of the order of 10^{-10} (relative 10^{-14}) for the mass, 10^{-10} (relative 10^{-15}) for the momentum, 10^{-2} (relative 10^{-15}) for the energy.

Similar considerations hold for the Le Blanc shock tube computations (Fig. 3), which supports what shown in Sec. 5.2: the van der Vegt's formula and the HLLC flux calculated using Formula (5) are identical. In passing we notice in Fig. 3 the classical low convergence speed toward the exact solution (as in [3, Fig. 9]), which is not due to the flux formulae.

7. Conclusion

In this short note we have proposed a formula which, on the one hand, can be applied to design/compute approximate Riemann solvers in the ALE formulation starting from their Eulerian version. On the other hand the same formula is also useful to verify the correctness of an ALE approximate Riemann solver using its Eulerian version. Using this formula, we have derived the AUSM$^+$ ALE version proposed in [6] and have shown that the HLLC solver for moving meshes, also proposed in [6], is not correct, as also supported by a numerical example.

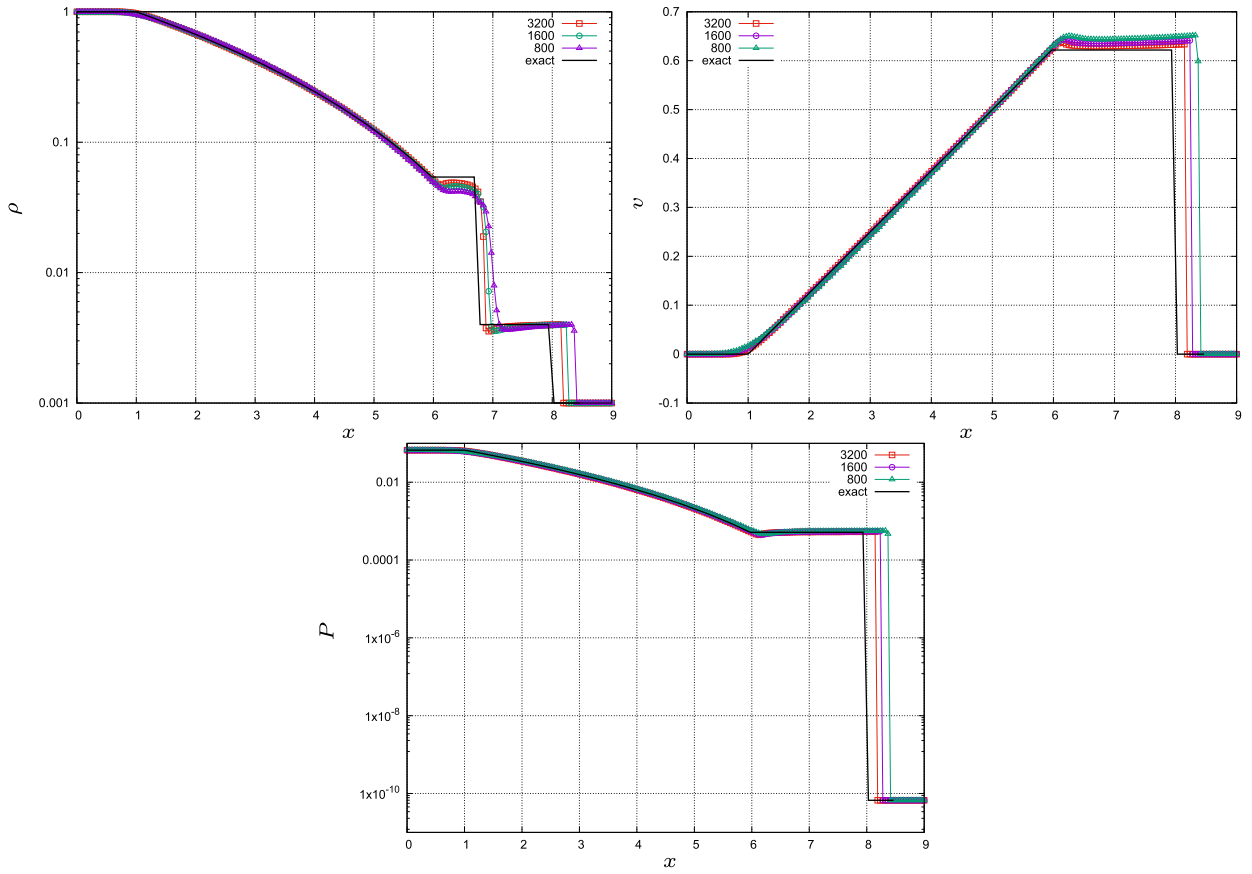

Fig. 3. Gas-water shock tube (Table 1, Case 3). SI values. HLLC computations with Formula (5).

CRediT authorship contribution statement

V. Chicu: Validation, Software, Methodology, Investigation, Conceptualization. **A. Beccantini:** Writing – original draft, Validation, Software, Methodology, Investigation, Conceptualization. **M. Gherardi:** Writing – review & editing, Investigation.

Declaration of competing interest

The authors declare that they have no known competing financial interests or personal relationships that could have appeared to influence the work reported in this paper.

Acknowledgements

This work has been mainly realized within the framework of the “Dynamique rapide” project of the CEA/EDF/Framatome tripartite institute, during Viorel Chicu’s visit at CEA Saclay. It has been achieved during his PhD at Alma Mater Studiorum-Universitá di Bologna, entitled “Assessment of a new model for the investigation of an hypothetical Steam Generator Tube Rupture accident in lead-cooled fast reactors” and funded by *new*cleo. The authors are very grateful to the reviewers of this short note for their many comments which, in our opinions, greatly improved readability. Special thanks to Nicolas Lelong for fruitful discussions.

Data availability

Data will be made available on request.

References

[1] S. Godunov, Finite difference method for numerical computation of discontinuous solutions of the equations of fluid dynamics, Mat. Sb. 47(89) (3) (1959) 271–306.
[2] E. Toro, Riemann Solvers and Numerical Methods for Fluid Dynamics, vol. 44, Springer-Verlag Berlin Heidelberg, 2009, arXiv:1011.1669v3.

[3] A. Chan, G. Gallice, R. Loubère, P.-H. Maire, Positivity preserving and entropy consistent approximate Riemann solvers dedicated to the high-order MOOD-based Finite Volume discretization of Lagrangian and Eulerian gas dynamics, Comput. Fluids 229 (2021) 105056, https://doi.org/10.1016/j.compfluid.2021.105056.
[4] J. Donea, A. Huerta, J. Ponthot, A. Rodríguez-Ferran, Arbitrary Lagrangian–Eulerian methods, https://doi.org/10.1002/0470091355.ecm009, Aug. 2004.
[5] A.J. Barlow, P.-H. Maire, W.J. Rider, R.N. Rieben, M.J. Shashkov, Arbitrary Lagrangian–Eulerian methods for modeling high-speed compressible multimaterial flows, J. Comput. Phys. 322 (2016) 603–665, https://doi.org/10.1016/j.jcp.2016.07.001.
[6] H. Luo, J.D. Baum, R. Löhner, On the computation of multi-material flows using ALE formulation, J. Comput. Phys. 194 (1) (2004) 304–328, https://doi.org/10.1016/j.jcp.2003.09.026.
[7] D.S. Balsara, J. Vides, K. Gurski, B. Nkonga, M. Dumbser, S. Garain, E. Audit, A two-dimensional Riemann solver with self-similar sub-structure – alternative formulation based on least squares projection, J. Comput. Phys. 304 (2016) 138–161, https://doi.org/10.1016/j.jcp.2015.10.013, http://linkinghub.elsevier.com/retrieve/pii/S0021999115006762.
[8] G. Gallice, A. Chan, R. Loubère, P.-H. Maire, Entropy stable and positivity preserving Godunov-type schemes for multidimensional hyperbolic systems on unstructured grid, J. Comput. Phys. 468 (2022) 111493, https://doi.org/10.1016/j.jcp.2022.111493.
[9] A. Beccantini, P. Galon, N. Lelong, F. Baj, Tangential artificial viscosity to alleviate the carbuncle phenomenon, with applications to single-component and multi-material flows, J. Comput. Phys. 516 (2024) 113369, https://doi.org/10.1016/j.jcp.2024.113369.
[10] M.-S. Liou, A sequel to AUSM, part II: AUSM+ -up for all speeds, J. Comput. Phys. 214 (1) (2006) 137–170, https://doi.org/10.1016/j.jcp.2005.09.020.
[11] Y. Wada, M.-S. Liou, An accurate and robust flux splitting scheme for shock and contact discontinuities, SIAM J. Sci. Comput. 18 (3) (1997) 633–657, https://doi.org/10.1137/S1064827595287626.
[12] P. Batten, N. Clarke, C. Lambert, D.M. Causon, On the choice of wavespeeds for the HLLC Riemann solver, SIAM J. Sci. Comput. 18 (6) (1997) 1553–1570, https://doi.org/10.1137/S1064827593260140.
[13] J. van der Vegt, H. van der Ven, Space–time discontinuous Galerkin finite element method with dynamic grid motion for inviscid compressible flows, J. Comput. Phys. 182 (2) (2002) 546–585, https://doi.org/10.1006/jcph.2002.7185.
[14] Europlexus, A computer program for the finite element-finite volume simulation of fluid-structure systems under transient dynamic loading, http://www-epx.cea.fr, December 2024.